Hyperbaric oxygen facilitates teniposide-induced cGAS-STING activation to enhance the antitumor efficacy of PD-1 antibody in HCC

Kun Li,[1] Yihang Gong,[1] Dongbo Qiu,[2] Hui Tang,[1] Jian Zhang,[1] Zenan Yuan,[1] Yingqi Huang,[3] Yunfei Qin,[3] Linsen Ye ![ORCID],[1] Yang Yang[1]

ABSTRACT

Background Emerging evidence indicates that the cyclic GMP-AMP synthase-stimulator of interferon genes (cGAS-STING) axis plays a pivotal role in intrinsic antitumor immunity. Previous studies demonstrate that the conventional chemotherapy agent, teniposide, effectively promotes the therapeutic efficacy of programmed cell death protein-1 antibody (PD-1 Ab) through robust cGAS-STING activation. Unfortunately, the cGAS expression of tumor cells is reported to be severely suppressed by the hypoxic status in solid tumor. Clinically, enhancing chemotherapy-induced, DNA-activated tumor STING signaling by alleviating tumor hypoxia might be one possible direction for improving the currently poor response rates of patients with hepatocellular carcinoma (HCC) to PD-1 Ab.

Methods Teniposide was first screened out from several chemotherapy drugs according to their potency in inducing cGAS-STING signaling in human HCC cells. Teniposide-treated HCC cells were then cultured under hypoxia, normoxia or reoxygenation condition to detect change in cGAS-STING signaling. Next, oxaliplatin/teniposide chemotherapy alone or combined with hyperbaric oxygen (HBO) therapy was administered on liver orthotopic mouse tumor models, after which the tumor microenvironment (TME) was surveyed. Lastly, teniposide alone or combined with HBO was performed on multiple mouse tumor models and the subsequent anti-PD-1 therapeutic responses were observed.

Results Compared with the first-line oxaliplatin chemotherapy, teniposide chemotherapy induced stronger cGAS-STING signaling in human HCC cells. Teniposide-induced cGAS-STING activation was significantly inhibited by hypoxia inducible factor 1α in an oxygen-deficient environment in vitro and the inhibition was rapidly removed via effective reoxygenation. HBO remarkably enhanced the cGAS-STING-dependent tumor type I interferon and nuclear factor kappa-B signaling induced by teniposide in vivo, both of which contributed to the activation of dendritic cells and subsequent cytotoxic T cells. Combined HBO with teniposide chemotherapy improved the therapeutic effect of PD-1 Ab in multiple tumor models.

Conclusions By combination of two therapies approved by the Food and Drug Administration, we safely stimulated an immunogenic, T cell-inflamed HCC TME, leading to further sensitization of tumors to anti-PD-1 immunotherapy. These findings might enrich therapeutic strategies for advanced HCC andwe can attempt to improve the response rates of patients with HCC to PD-1 Ab by enhancing DNA-activated STING signaling through effective tumor reoxygenation.

WHAT IS ALREADY KNOWN ON THIS TOPIC

⇒ Stimulator of interferon genes (STING) activation in the tumor microenvironment induced by agonists has been proven to result in potent tumor regression in multiple animal models.

⇒ Clinically, how to efficiently trigger tumor STING signaling via existing therapies or therapeutic combinations remains to be further described.

WHAT THIS STUDY ADDS

⇒ In this study, we verified that the combination of two therapies approved by the Food and Drug Administration, hyperbaric oxygen and teniposide chemotherapy, could synergistically trigger efficient tumor STING activation and eventually stimulate a robust adaptive antitumor immune response in hepatocellular carcinoma.

HOW THIS STUDY MIGHT AFFECT RESEARCH, PRACTICE OR POLICY

⇒ These findings might enrich therapeutic strategies for clinical practice and we can boost DNA-activated STING signaling by effective tumor reoxygenation.

INTRODUCTION

As an important signaling pathway of innate immunity, the cyclic GMP-AMP synthase-stimulator of interferon genes (cGAS-STING) axis has been revealed to play a pivotal role in intrinsic antitumor immunity in recent years.[1 2] When cGAS senses abnormal fragments of double-stranded DNA (dsDNA) in the cytoplasm, it catalyzes the synthesis of cyclic dinucleotides (CDNs) to initiate signal transduction. CDNs then bind to STING and the activated STING recruits TANK-binding

kinase 1 to subsequently activate both interferon regulatory factor 3 (IRF3) and nuclear factor kappa-B (NF-κB), eventually resulting in the secretion of interferon-α/β (IFN-α/β), proinflammatory cytokines and chemokines.[3–5] Together, these factors promote the recruitment and maturation of dendritic cells (DCs), leading to tumor infiltration and activation of cytotoxic T lymphocytes (CTLs).[6 7] Activation of the cGAS-STING axis inside the tumor microenvironment (TME) is an effective way to inhibit tumor growth; thus, many researchers attempt to directly inject CDNs (endogenous ligands for STING) into the tumors or develop novel types of potent exogenous STING agonists for oral or intravenous use.[8–10] Although these efforts exhibit ideal antitumor ability in various animal tumor models, they are only staying at the preclinical stages.[1]

Chemotherapy is routinely used in cancer treatment and could cause tumor cell DNA breaks and damages. Thus, chemotherapy might be a clinically applicable method to induce tumor cell-intrinsic STING activation.[1 11 12] Teniposide is a DNA topoisomerase II inhibitor mainly used for treatment of lymphoma and glioblastoma. As a traditional chemotherapy agent, teniposide was recently demonstrated to induce efficient cGAS-STING signaling in multiple tumor models.[13] Considering the poor efficacy of the chemotherapy regimen currently used for hepatocellular carcinoma (HCC),[14] we were eager to know whether teniposide has potential therapeutic prospect in HCC chemotherapy.

As a major cytosolic DNA sensor, cGAS is responsible for the initiation of cGAS-STING type I interferon (IFN-I) signal transduction. Unfortunately, cGAS expression was reported to be suppressed in the oxygen-deficient environment in breast cancer, allowing tumor cells to escape immunological responses induced by damage-associated molecular pattern molecules.[15] Thus, restoring cGAS expression in tumor cells by overcoming the anoxic status inside the TME might be a potential antitumor strategy. As HCC is a solid tumor characterized by severe TME hypoxia,[16] we aim to determine whether tumor cGAS-STING activation could be promoted by alleviating tumor hypoxia in HCC.

Hyperbaric oxygen (HBO) has been used in clinical practice for many years. When operating at an elevated air pressure, generally 2.5–3 atmosphere absolute (ATA), HBO can safely increase the partial pressure of blood oxygen and facilitate tissue oxygen delivery in a non-invasive manner.[17] As a conventional therapy, HBO has attracted much attention in cancer treatment in recent years.[18–20] Here, to maximize cGAS-STING activation in HCC, we combined two therapies approved by the Food and Drug Administration (FDA): teniposide and HBO. By implementing teniposide chemotherapy, we achieved stronger STING activation than routine HCC chemotherapy drugs. By subsequently repeated HBO administration, we further enhanced the cGAS-STING signaling induced by teniposide chemotherapy. Thus, the combination of HBO with teniposide synergistically activated the antitumor immune response in HCC and sensitized tumor response to antiprogrammed cell death protein-1 (anti-PD-1) immunotherapy.

METHODS AND MATERIALS
Mice, cell lines and reagents
Six-week-old male C57BL/6J mice were purchased from the Model Animal Research Center of Nanjing University (China). All mice were raised under specific pathogen-free conditions.

The Hep3B, Huh7, THP-1, Hepa1-6, MC38, B16 and HEK293 cell lines were obtained from ATCC. All cells were tested negative for mycoplasma. Cells were cultured with either high-glucose Dulbecco's Modified Eagle's Medium (DMEM) (Gibco) or Roswell Park Memorial Institute (RPMI)-1640 (Gibco), supplemented with 10% fetal bovine serum (FBS) (PAN-Biotech) at 37°C in 5% CO_2. Hypoxia culture was conducted in a hypoxic incubator (New Brunswick Galaxy 48R) at 1% O_2, 5% CO_2 and 94% N_2.

The following chemical reagents were used in this study: Lipofectamine 3000 (Invitrogen, L3000015), herring testes (HT) DNA (Sigma-Aldrich, D6898), teniposide (MCE, HY-13761), oxaliplatin (MCE, HY-17371), cisplatin (MCE, HY-17394), doxorubicin (MCE, HY-15142), sorafenib (MCE, HY-10201) and 5-fluorouracil (MCE, HY-90006).

Immunoblotting
The procedure for immunoblotting analyses was performed as previously described.[21] The following antibodies were used for immunoblotting analyses: cGAS (Novus, NBP1-86761), IRF3 (HUABIO, ET1612-14), P65 (CST, 6956), p-IRF3 (Abcam, ab76493), p-P65 (CST, 3033), HIF-1α (CST, 14179), β-actin (Santa Cruz, sc-47778), anti-mouse IgG (CST, 7076) and anti-rabbit IgG (CST, 7074). Protein bands were visualized by a Tanon 5200 chemiluminescence image analysis system (China).

Immunohistochemistry and immunofluorescence
For immunohistochemistry (IHC), slides of tumor sections were prepared as previously described.[21] Sections were incubated with primary antibodies against p-IRF3 (CST, 29047), CD11c (CST, 97585), CD8 (Abcam, ab217344) and HIF-1α (Abcam, ab114977) at 4°C overnight. After incubation with a secondary antibody (Dako) for 1 hour at 37°C, the signal was revealed by the DAB Chromogenic Kit (Dako).

For immunofluorescence, tumor tissues were prepared as described for IHC and sections were incubated with primary antibodies against p-IRF3 (CST, 29047) and HIF-1α (Santa Cruz, sc-13515) at 4°C overnight. After washing with phosphate buffered saline (PBS), sections were incubated with CF488-conjugated goat-anti-rabbit IgG (Biotium, 20019) or CF568-conjugated goat-anti-mouse IgG (Biotium, 20101) at room temperature for 1 hour. The

nuclei were revealed by 4′,6-diamidino-2-phenylindole (DAPI) (Sigma-Aldrich, D9542) staining. Fluorescence images were collected using a fluorescence microscope (Leica DM4000B, Germany).

Multiplex immunohistochemistry (mIHC) staining was performed using tyramide signal amplification (TSA) Plus Fluorescence Kits (PerkinElmer, USA) combined with IHC (TSA-IHC). Various primary antibodies, including p-IRF3 (CST, 29047), CD11c (CST, 97585), CD3 (Abcam, ab16669) and CD8 (Abcam, ab217344), were sequentially applied at 37°C for 1 hour, followed by horseradish peroxidase-conjugated secondary antibody incubation and TSA. The slides were microwave heat-treated after each TSA operation. The nuclei were counterstained with DAPI and images were acquired using tissue FAXS SL spectra (TissueGnostics, Austria).

Real-time PCR and ELISA analysis
The total RNA of tumor cells and tumor tissues was extracted using an RNA Quick Purification Kit (Yishan Biotech) according to the manufacturer's instructions. The RNA was then reverse-transcribed to complementary DNA (cDNA) using HiScript III RT SuperMix for real time quantitative PCR (RT-qPCR) with gDNA wiper (Vazyme, R323-01). SYBR Green III (Vazyme, Q711-02/03) was used for the RT-qPCR of non-TaqMan primers, and Universal Master Mix II with UNG (Thermo Fisher, 4440038) was used for the RT-PCR of TaqMan primers. The primer sequences are listed in online supplemental table 1.

Supernatant levels of human IFN-β (R&D Systems, DIFNB0) and mouse IFN-β (R&D Systems, MIFNB0) were measured by ELISA kits following the manufacturer's instructions.

Flow cytometry analysis
Fluorochrome-labeled antibodies employed in flow cytometry were used according to the manufacturer's protocol. The following antibodies were used for cell staining: calreticulin (CST, 62304), PD-L1 (BD, 563741), CD4 (Biolegend, 100411), CD8a (BD, 561095), F4/80 (BD, 565787), CD11b (Biolegend, 101207), CD11c (BD, 562949), CD86 (Biolegend, 105013), CD206 (Biolegend, 141703), MHC-I (Biolegend, 114613), MHC-II (Biolegend, 107627), IFN-γ (BD, 560660), TNF-α (BD, 563387), granzyme B (Biolegend, 372206) and Ki67 (Biolegend, 652410). Fluorescence data were acquired on a BD LSRFortessa cytometer and analyzed using FlowJo V.X.

shRNA knockdown
The expression of *cGAS*, *STING* and *HIF1A* was knocked down by the indicated short hairpin RNA (shRNA) in HCC tumor cells. Briefly, shRNA lentiviral vectors were cotransfected with psPAX2 and pMD2.G packaging plasmids into 293T cells. The supernatants were harvested 48 hours after transfection and used for infection of tumor cells followed by puromycin selection for 2 days. The knockdown effect was assessed by immunoblotting using cellular protein extracts. The shRNA sequences are listed in online supplemental table 1.

HBO therapy
The experimental HBO chamber was manufactured by Shanghai 701 Yang Garden Hyperbaric Oxygen Chamber (Shanghai, China). Mice labeled by group were placed into the HBO chamber and the door of the chamber was tightly closed. The chamber was ventilated with high-flow 100% oxygen before pressurization. The oxygen concentration in the chamber was monitored by an oximeter. During HBO therapy, the oxygen concentration and air pressure in the chamber were consistently maintained above 90% and 2.8 ATA, respectively, for 2 hours by continuous low-flow oxygen ventilation. At least 10 min of pressurization and 20 min of depressurization were required to allow the mice to adapt to the rapid air pressure changes.

In vivo tumor experiments
For TME survey experiments, Hepa1-6 cells suspended in PBS were mixed with Matrigel matrix (Corning, 354234) in a volume ratio of 2:1 and tumor cells (1×10^6 cells per 50 µL) were orthotopically inoculated into the hepatic subcapsular of the right liver lobe of B6 mice. Tumors were allowed to grow for 5 days and the mice were then treated with DMSO (Ctrl), teniposide (10 mg/kg, intraperitoneal injection), oxaliplatin (10 mg/kg, intraperitoneal injection), HBO, HBO+oxaliplatin and HBO+teniposide at the indicated time points (n=3 per group).

For anti-PD-1 sensitization experiments, 100 µL of Matrigel matrix premixed with Hepa1-6, MC38 or B16 cells were subcutaneously injected into the left flank of B6 mice (0.5×10^6 cells per mouse). Tumors were allowed to grow for 5 days and the mice were then treated with DMSO (Ctrl), teniposide (10 mg/kg, intraperitoneal injection) or HBO+teniposide at the indicated time points, followed by three intraperitoneal injections of PD-1 antibody (Ab) (Bio X Cell, 200 µg per mouse) every 3 days (n=5 per group). Tumor diameter was measured by a vernier caliper and tumor volume was calculated as: V (mm^3)=0.5 × tumor length (mm) × (tumor width, in mm)^2.

Safety evaluation
Serum samples and the major organs of tumor-bearing mice in each group were obtained after treatment withdrawal. Blood biochemical parameters were analyzed by an automatic analyzer (Hitachi 3100, Japan). The major organs were fixed for H&E staining to assess pathological changes.

Patient sample collection and evaluation of IHC
Fresh clinical tumor samples were acquired from three patients with HCC who underwent open hepatectomy at the Third Affiliated Hospital, Sun Yat-sen University. Samples for IHC were collected from 120 patients who underwent laparoscopic or open hepatectomy at the Third Affiliated Hospital, Sun Yat-sen University from

January 2013 to December 2016. None of these patients had received antitumor therapy before surgery. Informed consent forms were signed by all study participants.

The staining intensity of tumor p-IRF3 expression was scored as 0 (negative), 1 (weak), 2 (moderate) or 3 (high). The percentage of positive cells was categorized as 0 (0%), 1 (1%–25%), 2 (26%–50%), 3 (51%–75%) or 4 (76%–100%). The IHC staining score was blindly calculated by different individuals using the staining intensity multiplied by the positive cell percentage. Staining scores between 0 and 5 were defined as p-IRF3 low expression and scores between 6 and 12 were considered as p-IRF3 high expression.

Statistical analysis
GraphPad Prism V.7 and IBM SPSS Statistics V.24 were used to analyze the data. Comparisons between two groups were analyzed using a two-tailed unpaired Student's t-test. Cox regression analysis with the log-rank test was performed to determine overall survival (OS) and disease-free survival (DFS). Statistical significance was defined as a p value less than 0.05.

RESULTS
Teniposide robustly activates the cGAS-STING axis in human HCC cells
Several chemotherapy drugs have been reported to induce the damage and leakage of nuclear DNA in tumor cells, which are sensed by cytosolic DNA sensors, thereby triggering downstream innate immune signaling. Although teniposide has been proven to effectively induce IFN-I and NF-κB signaling in various mouse tumor models via the cGAS-STING activation, whether it works in human HCC remains to be determined. To verify the innate immune signaling inductive potency of teniposide in human HCC cells, we selected sorafenib, doxorubicin, 5-fluorouracil, cisplatin and oxaliplatin, which are commonly used systemic or local chemotherapy drugs in HCC treatment, for comparison. We treated Hep3B and Huh7 cells with these drugs at their respective 50% inhibitory concentration for 24 hours (online supplemental figure 1A). We then detected the cellular protein levels of p-IRF3 and p-P65, two pivotal transcription factors for inducing IFN-I and NF-κB signaling. The results showed that teniposide induced the strongest p-IRF3 and p-P65 expression among these six drugs tested in human HCC cells (online supplemental figure 1B).

Because oxaliplatin is the major component of the first-line HCC chemotherapy regimen recommended by the National Comprehensive Cancer Network,[14 22] we next compared teniposide with oxaliplatin in detail in terms of innate immune signaling induction in human HCC cells. Consistent with the cellular p-IRF3 and p-P65 protein expression levels, teniposide treatment significantly increased the IFN-β secretion and the mRNA expression of *IFIT1*, *IFIT2*, *CCL5* and *CXCL10* in Hep3B and Huh7 cells (figure 1A–C). These data further confirmed

the robust activation of IFN-I and NF-κB signaling in human HCC cells after teniposide chemotherapy, but not oxaliplatin. As IFN-I and NF-κB signalings could be induced via multiple pathways, including the cGAS-STING pathway, the RIG-I-MAVS pathway and the Toll-like receptor pathway, we knocked down *cGAS* or *STING* in HCC cells using shRNA and observed that teniposide-induced p-IRF3 and p-P65 expressions were significantly weakened in the cGAS-STING-deficient cells (figure 1D,E and online supplemental figure 2A,B). These data indicate the activation of IFN-I and NF-κB signaling in human HCC cells induced by teniposide depended on the cGAS-STING axis. Furthermore, we also detected the increased expression of two immunogenic cell death (ICD) biomarkers, namely calreticulin and programmed cell death ligand 1 (PD-L1), after teniposide treatment (online supplemental figure 2C,D), indicating teniposide might also induce stronger ICD effects in human HCC cells than oxaliplatin.

These data showed that, in addition to inhibiting the proliferation of tumor cells, teniposide robustly activated cGAS-STING-dependent IFN-I and NF-κB signaling in human HCC cells, suggesting that teniposide might serve as a potential chemotherapeutic drug in HCC treatment, especially when combined with immune checkpoint inhibitors (ICIs).

Hypoxia inhibits teniposide-induced cGAS-STING activation by suppressing cGAS expression in human HCC cells
A previous study has revealed that hypoxia suppressed cGAS expression in breast cancer cells.[15] As hypoxia is a prominent hallmark of the HCC TME, we thus verified this phenotype in human HCC cells. First, we cultured tumor cells under a normoxic (21% O_2) or a hypoxic (1% O_2) condition and observed that hypoxic culture attenuated cGAS expression in human HCC cells (figure 2A). To further determine the influence of hypoxia on the downstream signal transduction of cGAS, we next transfected HCC cells with HT-DNA before hypoxic culture and found that p-IRF3 expression was remarkably decreased under oxygen-deficient conditions, indicating that hypoxia inhibited DNA-induced cGAS-STING activation in human HCC cells (figure 2B). Similarly, we also observed the inhibition of cGAS expression and downstream p-IRF3 activation in THP-1 human mononuclear immune cells under hypoxia (online supplemental figure 3A).

Because teniposide induced potent innate immune signaling in a cGAS-dependent manner, we next investigated the effects of hypoxia on the IFN-I and NF-κB signaling induction after teniposide treatment. Consistent with the results of HT-DNA transfection, lower cellular p-IRF3 protein expression and IFN-β secretion, decreased interferon-stimulated genes (ISG) mRNA expression indicated that hypoxia markedly suppressed the activation of IFN-I signaling induced by teniposide (figure 2C–E). Furthermore, cellular p-P65 protein and chemokine mRNA expressions were also significantly
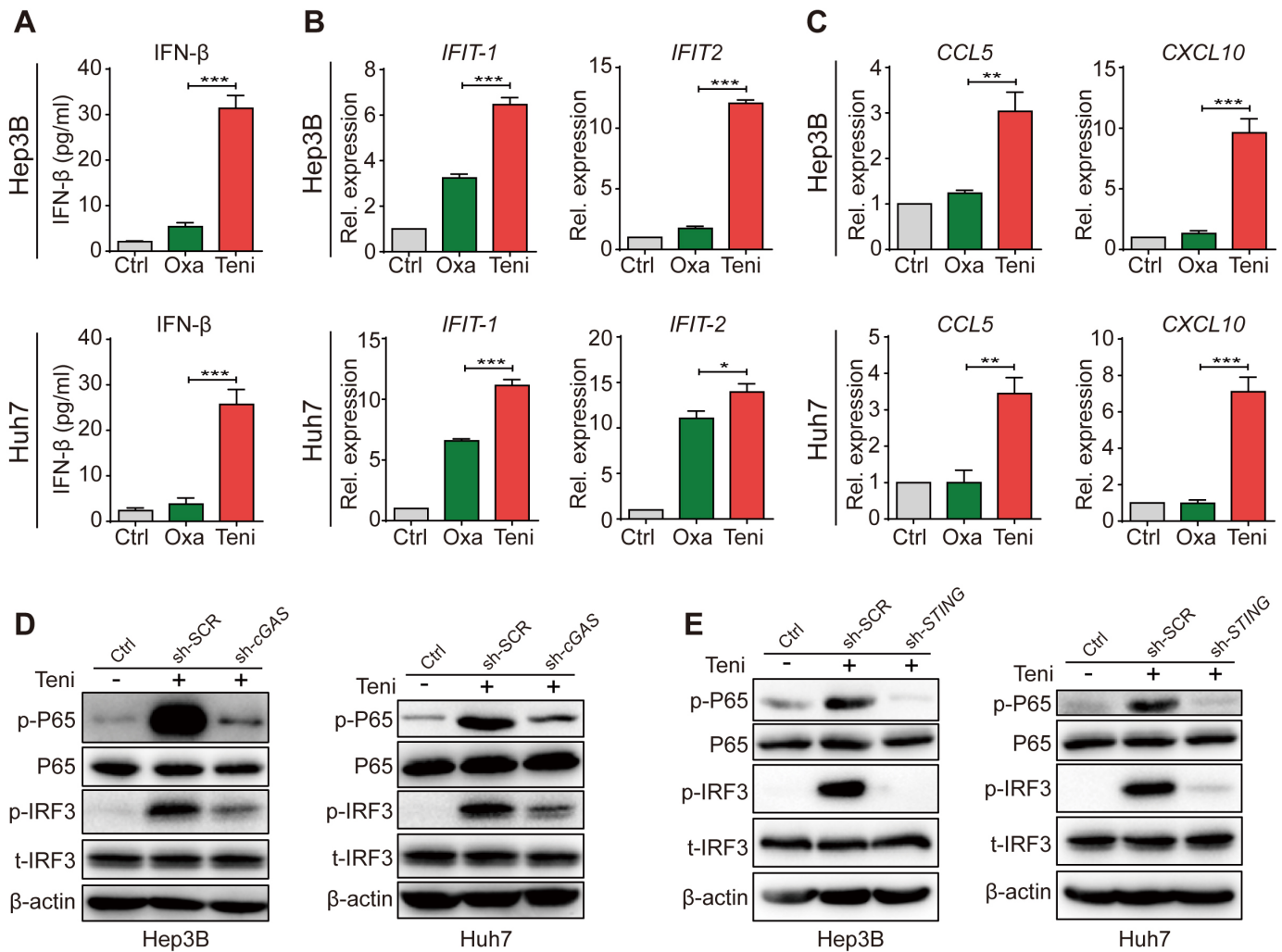
Figure 1 Teniposide triggered type I interferon and NF-κB signaling through the cGAS-STING activation in human HCC cells. (A–C) Hep3B and Huh7 cells were treated with oxaliplatin or teniposide at each IC50 for 24 hours and the supernatant IFN-β was then measured by ELISA (A) and the mRNA expression of *IFIT-1* and *IFIT-2* (B) and *CCL5* and *CXCL10* (C) was measured by RT-qPCR. (D) Hep3B and Huh7 cells transduced with *cGAS*-shRNA or scramble-shRNA were treated with teniposide at each IC50 for 24 hours and the cellular protein expression of p-IRF3 and p-P65 was then detected by immunoblotting; β-actin was used as a loading control. (E) Hep3B and Huh7 cells transduced with *STING*-shRNA or scramble-shRNA were treated as in (D) and the cellular protein expression of p-IRF3 and p-P65 was then detected by immunoblotting. Data in (D) and (E) are representative of three independent experiments. Data in (A), (B) and (C) are shown as mean±SD of three independent experiments. *P<0.05, **P<0.01, ***P<0.001. cGAS-STING, cyclic GMP-AMP synthase-stimulator of interferon genes; Ctrl, control; HCC, hepatocellular carcinoma; IC50, 50% inhibitory concentration; IFN-β, interferon β; IRF3, interferon regulatory factor 3; NF-κB, nuclear factor kappa-B; Oxa, oxaliplatin; Rel. expression, relative expression; RT-qPCR, real time quantitative PCR; sh-SCR, short hairpin RNA-scrambled; sh-cGAS, short hairpin RNA-cGAS; Teni, teniposide.

restricted under hypoxia (figure 2C,F). Additionally, we also observed that hypoxia inhibited teniposide-induced IFN-β secretion in multiple murine tumor cell lines (online supplemental figure 3B–D). Together, these data illustrate the negative influence of hypoxia on cGAS-STING activation induced by teniposide chemotherapy in human HCC cells.

Reoxygenation promotes teniposide-induced cGAS-STING activation by rescuing cGAS expression in human HCC cells

We next investigated the dynamic change of cGAS expression in human HCC cells when the oxygen-deficient status was removed. We reoxygenated tumor cells by transferring culture flasks from hypoxic conditions to normoxic conditions and observed that, with the degradation of hypoxia inducible factor 1α (HIF-1α), cGAS expression was rapidly rescued within 8 hours (figure 3A). As a consequence, teniposide-induced cGAS-STING activation was also promoted by reoxygenation as cellular p-IRF3 and p-P65 protein levels, IFN-β secretion levels, and ISG mRNA and chemokine mRNA expression levels in the reoxygenation group were notably higher than those in the absolute hypoxia group (figure 3B–D).

As HIF-1α is a key transcription factor that plays a crucial role in the cellular response to hypoxia, we thus investigated whether HIF-1α mediates the suppression of cGAS-STING activation under hypoxia. Knockdown
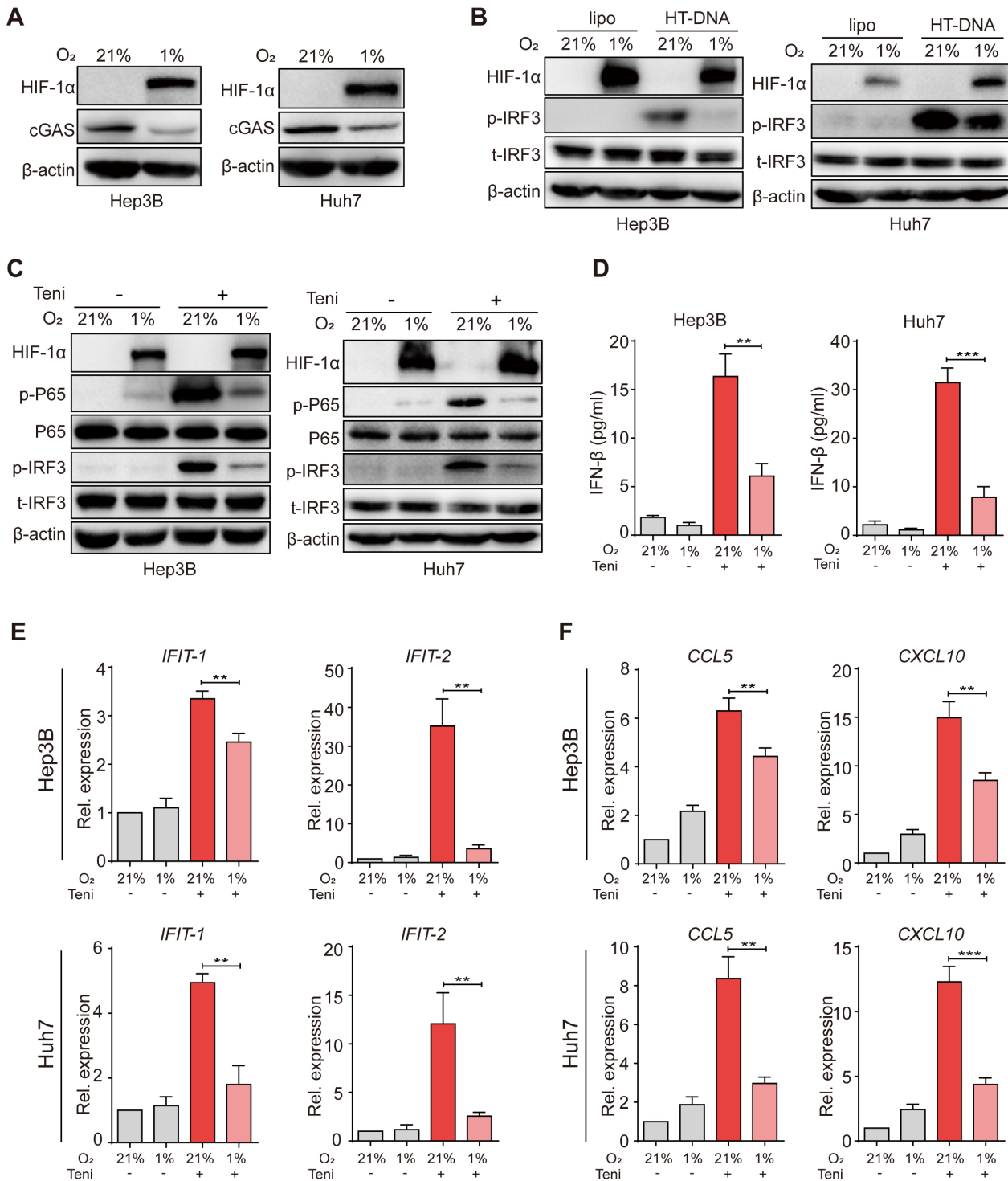
Figure 2 Hypoxia inhibited teniposide-induced cGAS-STING activation in human HCC cells. (A) Hep3B and Huh7 cells were cultured under a normoxic (21% O_2) or a hypoxic (1% O_2) condition for 18 hours and the cellular protein expression of HIF-1α and cGAS was then detected by immunoblotting; β-actin was used as a loading control. (B) Hep3B and Huh7 cells were transfected with HT-DNA (5 μg/mL) and the cells were then cultured under either normoxic or hypoxic condition for 24 hours; the cellular protein expression of p-IRF3 was detected by immunoblotting. (C) Hep3B and Huh7 cells were treated with teniposide at each IC50, followed by either normoxic or hypoxic culture for 24 hours, and the cellular protein expression of p-IRF3 and p-P65 was then detected by immunoblotting. (D) Hep3B and Huh7 cells were treated as in (C) and the supernatant IFN-β was then measured by ELISA. (E–F) Hep3B and Huh7 cells were treated as in (C) and the mRNA expression of *IFIT-1* and *IFIT-2* (E) and *CCL5* and *CXCL10* (F) was then measured by RT-qPCR. Data in (A), (B) and (C) are representative of three independent experiments. Data in (D), (E) and (F) are shown as mean±SD of three independent experiments. *P<0.05, **P<0.01,***P<0.001. cGAS-STING, cyclic GMP-AMP synthase-stimulator of interferon genes; HCC, hepatocellular carcinoma; HIF-1α, hypoxia inducible factor 1α; HT-DNA, herring testes-DNA; IC50, 50% inhibitory concentration; IFN-β, interferon β; IRF3, interferon regulatory factor 3; Rel. expression, relative expression; RT-qPCR, real time quantitative PCR; Teni, teniposide.
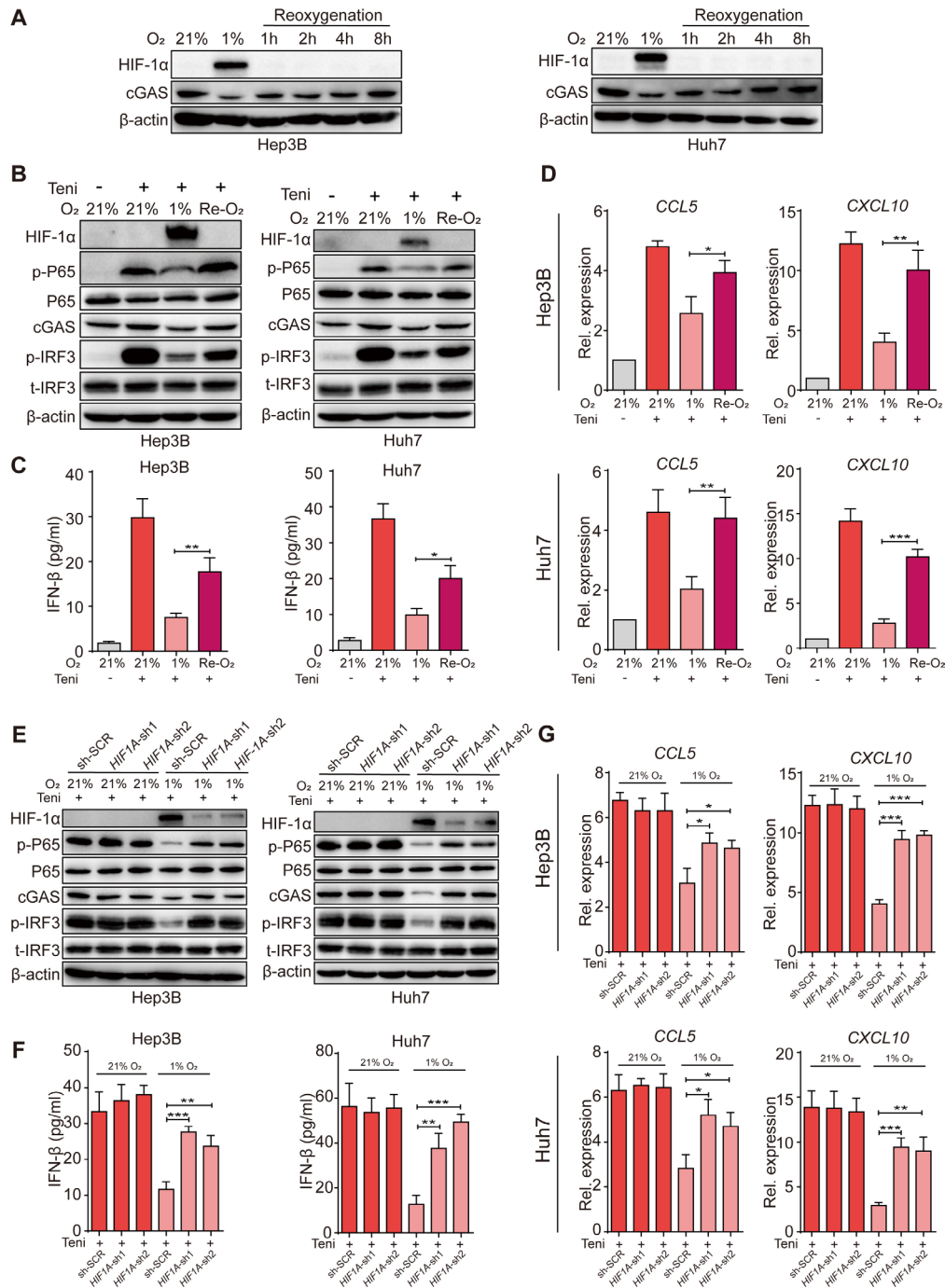
Figure 3 Reoxygenation restored teniposide-induced cGAS-STING activation in human HCC cells. (A) Hep3B and Huh7 cells were cultured under either a normoxic (21% O$_2$) or a hypoxic (1% O$_2$) condition for 18 hours and the cells were then transferred to normoxic (21% O$_2$) culture for 1 hour, 2 hours, 4 hours and 8 hours, respectively; the cellular protein expression of HIF-1α and cGAS was detected by immunoblotting at indicated time points and β-actin was used as a loading control. (B–D) Hep3B and Huh7 cells were treated with teniposide at each IC50, followed by hypoxic culture for 18 hours, and the cells were then transferred to normoxic culture for another 6 hours, and the cellular protein expression of p-IRF3 and p-P65 was detected by immunoblotting (B), the supernatant IFN-β was measured by ELISA (C), and the mRNA expression of *CCL5* and *CXCL10* was measured by RT-qPCR (D). (E–G) Hep3B and Huh7 cells transduced with *HIF1A*-shRNA or scramble-shRNA were treated with teniposide at each IC50, followed by either normoxic or hypoxic culture for 24 hours and the cellular protein expression of p-IRF3 and p-P65 was then detected by immunoblotting (E), the supernatant IFN-β was measured by ELISA (F), and the mRNA expression of *CCL5* and *CXCL10* was measured by RT-qPCR (G). Data in (A), (B) and (E) are representative of three independent experiments. Data in (C), (D), (F) and (G) are shown as mean±SD of three independent experiments. *P<0.05, **P<0.01, ***P<0.001. cGAS-STING, cyclic GMP-AMP synthase-stimulator of interferon genes; HCC, hepatocellular carcinoma; HIF-1α, hypoxia inducible factor 1α; IC50, 50% inhibitory concentration; IFN-β, interferon β; IRF3, interferon regulatory factor 3; Rel. expression, relative expression; RT-qPCR, real time quantitative PCR; sh-SCR, short hairpin RNA-scrambled; Teni, teniposide.

of *HIF1A* in human HCC tumor cells using shRNA abolished the hypoxia-induced suppression of cGAS, and as a result downstream p-IRF3 and p-P65 activation induced by teniposide was also rescued (figure 3E). Accordingly, teniposide-induced IFN-β secretion and ISG mRNA and chemokine mRNA expressions were all restored when *HIF1A* expression was silenced in human HCC cells (figure 3F,G).

These data suggest that the inhibition of cGAS-STING activation by hypoxia was dependent on HIF-1α and that reoxygenation promoted teniposide-induced IFN-I and NF-κB signaling by rapidly restoring cGAS-STING activation in human HCC cells.

HBO facilitates teniposide-induced activation of cGAS-STING in a mouse HCC tumor model

Our observations confirmed that hypoxia significantly suppressed teniposide-induced cGAS-STING activation, which was restored if the hypoxic condition was removed. To overcome the oxygen-deficient environment inside the tumor, we conducted repeated HBO therapy to a mouse HCC model and then evaluated the therapeutic effect and cGAS-STING signaling induction of oxaliplatin and teniposide chemotherapy after TME reoxygenation.

Hepa1-6 tumor cells were orthotopically transplanted into C57BL/6J mouse liver and the tumor-bearing mice were then randomly divided into six groups as follows: DMSO (Ctrl), hyperbaric oxygen (HBO), oxaliplatin chemotherapy (Oxa), teniposide chemotherapy (Teni), HBO+oxaliplatin (HBO+Oxa) and HBO+teniposide (HBO+Teni). The brief treatment schedule is described in figure 4A. Body weights were monitored daily when treatment started (online supplemental figure 4A). After the final HBO administration, all mice were sacrificed and orthotopic tumors were excised and weighed. The tumor weights of the control group and the HBO group were significantly higher than those of the chemotherapy groups, and HBO therapy alone did not affect tumor growth. Groups receiving oxaliplatin or teniposide chemotherapy showed an obvious tumor inhibition effect; however, HBO did not observably enhance the tumor inhibition effect of both chemotherapy drugs in the combination treatment groups by the end of the experiment (online supplemental figure 4B,C).

Serum biochemical parameters including alanine transaminase, aspartate aminotransferase, creatinine and blood urea nitrogen of the mice in each group were all within the normal ranges (online supplemental figure 4D-F). Histological examinations also showed no histopathological lesions in the major organs of mice receiving combined HBO and chemotherapy (online supplemental figure 4G). These results confirmed that HBO treatment did not increase the toxicity of both chemotherapeutic drugs.

By further analyzing the tumor tissues of each treatment group, we observed the notable degradation of tumor HIF-1α in the HBO group, indicating the definite removal of tumor hypoxia after HBO administration (figure 4B,C). Therefore, we next investigated tumor cGAS-STING

signaling after TME reoxygenation using the p-IRF3 expression level as an indicator based on our previous results. Using immunohistochemical staining, we observed stronger tumor p-IRF3 expression in the HBO+teniposide group than that in the teniposide chemotherapy group, suggesting that HBO helped teniposide to effectively trigger tumor cGAS-STING signaling. However, both the oxaliplatin chemotherapy group and the HBO+oxaliplatin group exhibited lower p-IRF3 expression than the groups containing teniposide chemotherapy (figure 4D). Consistently, we also detected significantly increased *Ifn-b*, *Ccl5* and *Cxcl10* mRNA expression in the tumor tissues of the HBO+teniposide group (figure 4E).

To evaluate the correlation between tumor p-IRF3 expression and the prognosis of HCC, we conducted Cox regression analyses to examine the prognostic impact of tumor p-IRF3 expression level for 120 patients with HCC (online supplemental table 2). Notably, higher tumor p-IRF3 expression level was associated with prolonged OS and DFS in patients with HCC (figure 4F,G). Using publicly available microarray databases of human patients, including the Gene Expression Omnibus, The Cancer Genome Atlas and the European Genome-phenome Archive, we further verified that higher expression of *HIF1A* was correlated with worse prognosis while higher expression of *IFNB1*, *CCL5* and *CXCL10* indicated better survival in patients with HCC (figure 4H,I).

These data demonstrate that by alleviating tumor hypoxia effectively, HBO therapy facilitated the cGAS-STING activation induced by teniposide chemotherapy in a mouse HCC tumor model. Therapeutic methods which could restrict tumor HIF-1α expression or promote tumor cGAS-STING activation might bring a better prognosis for patients with HCC.

HBO synergizes with teniposide chemotherapy to activate the antitumor response in a mouse HCC tumor model

Our results showed that although a higher p-IRF3 expression level did not significantly inhibit tumor growth in a rodent tumor model, it was associated with better prognosis in patients with HCC, suggesting that p-IRF3 expression might affect the TME in the long term. It is widely accepted that sufficient IFN-I signaling in TME plays an essential and sufficient role to bridge innate and adaptive antitumor immune responses, which is necessary for the recruitment and activation of proinflammatory immunocytes.[23 24] Using multiplex immunohistochemistry (mIHC), we also verified in human HCC tissues that large numbers of CD11c+ cells and CD8+ T cells accumulated in regions with high p-IRF3 expression. In contrast, few immune cells were recruited in the adjacent p-IRF3 low expression regions (figure 5A). This prompted us to further evaluate the immunocellular composition of the Hepa1-6 HCC TME of the mice from each treatment group.

First, we examined the tumor infiltration of innate immune cells including macrophages and DCs in each treatment group. We observed that HBO promoted the recruitment of macrophages into the tumor after
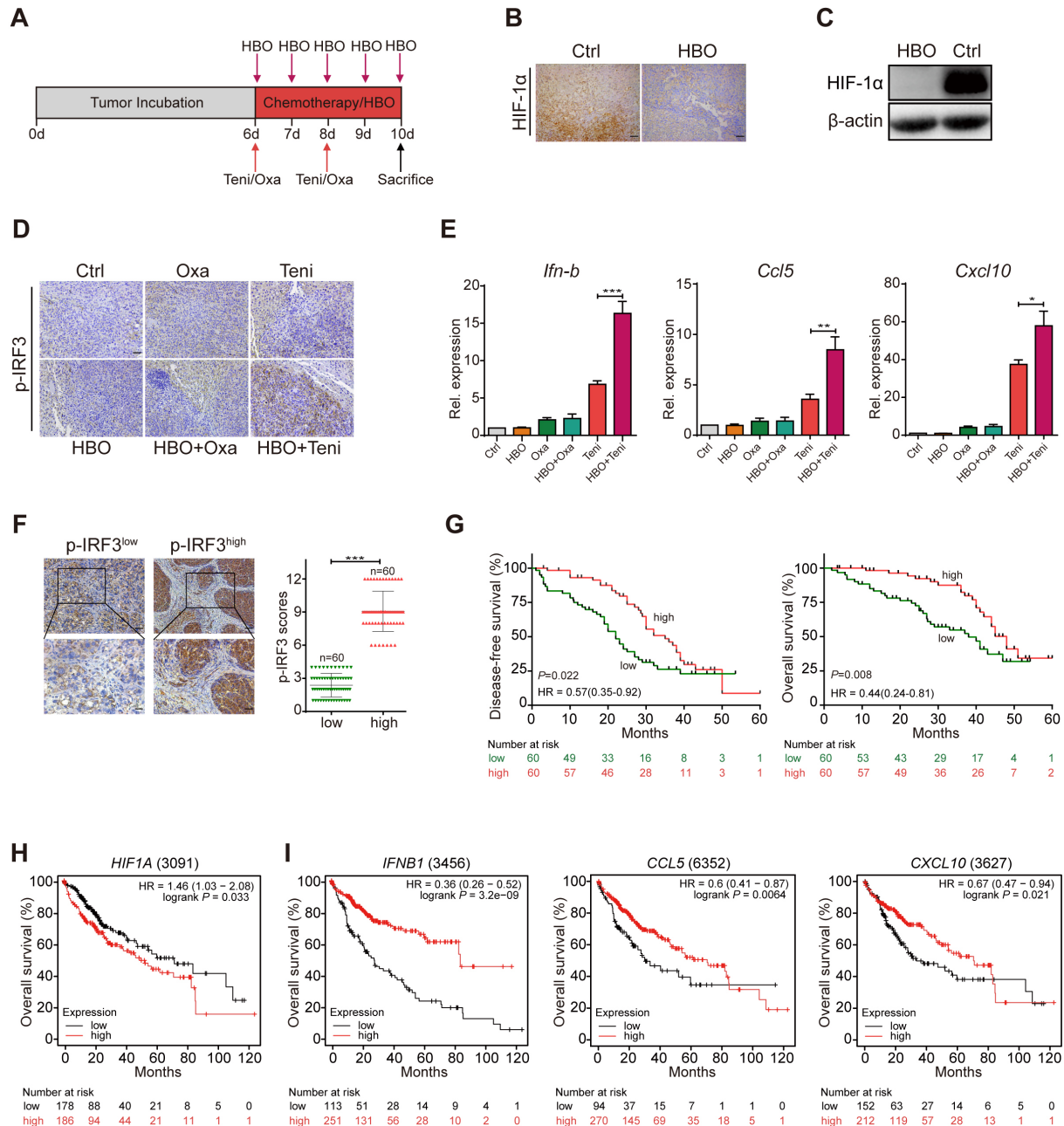
Figure 4 HBO facilitated teniposide to induce cGAS-STING signaling in mouse HCC tumor model. (A) Schematic illustration of the tumor microenvironment survey experiments in mouse HCC tumor model. Hepa1-6 liver orthotopically tumor-bearing mice were intraperitoneally injected with DMSO (Ctrl), oxaliplatin (10 mg/kg) and teniposide (10 mg/kg) twice at indicated time points. HBO therapy was administrated alone or after chemotherapy for a total of five times (n=3 per group). Tumors were resected and weighed after the final HBO administration. (B–C) HIF-1α expression of mice tumor tissues was determined by immunohistochemical staining (B) and immunoblotting (C) after HBO administration. Scale bars: 50 µm. (D) p-IRF3 expression of mice tumor tissues from different treatment groups was determined by immunohistochemical staining. Scale bars: 50 µm. (E) *Ifn-b*, *Ccl5* and *Cxcl10* mRNA expression of mice tumor tissues from different treatment groups was detected by RT-qPCR. (F) Representative images and quantitative analysis of p-IRF3^low (n=60) and p-IRF3^high (n=60) staining in tumor tissues from 120 patients with HCC. Scale bars: 50 µm (upper) and 25 µm (lower). (G) Disease-free survival (left) and overall survival (right) analyses of 120 patients with HCC showed a positive correlation between high p-IRF3 expression level and favorable prognosis. The prognostic significance was assessed by Cox regression analysis. (H–I) Kaplan–Meier curves were generated from the public microarray databases of human patients using an online software (kmplot.com/analysis/). Low expression levels of *HIF1A* (H) and high expression levels of *IFN-B1*, *CCL5* and *CXCL10* (I) were positively correlated with better survival of patients with HCC. Data in (C) are representative of three independent experiments. Data in (E) are shown as mean±SD of three independent experiments. *P<0.05, **P<0.01, ***P<0.001. cGAS-STING, cyclic GMP-AMP synthase-stimulator of interferon genes; Ctrl, control; HBO, hyperbaric oxygen; DMSO, Dimethyl sulfoxide; HCC, hepatocellular carcinoma; HIF-1α, hypoxia inducible factor 1α; IRF3, interferon regulatory factor 3; Oxa, oxaliplatin; Rel. expression, relative expression; RT-qPCR, real time quantitative PCR; Teni, teniposide.
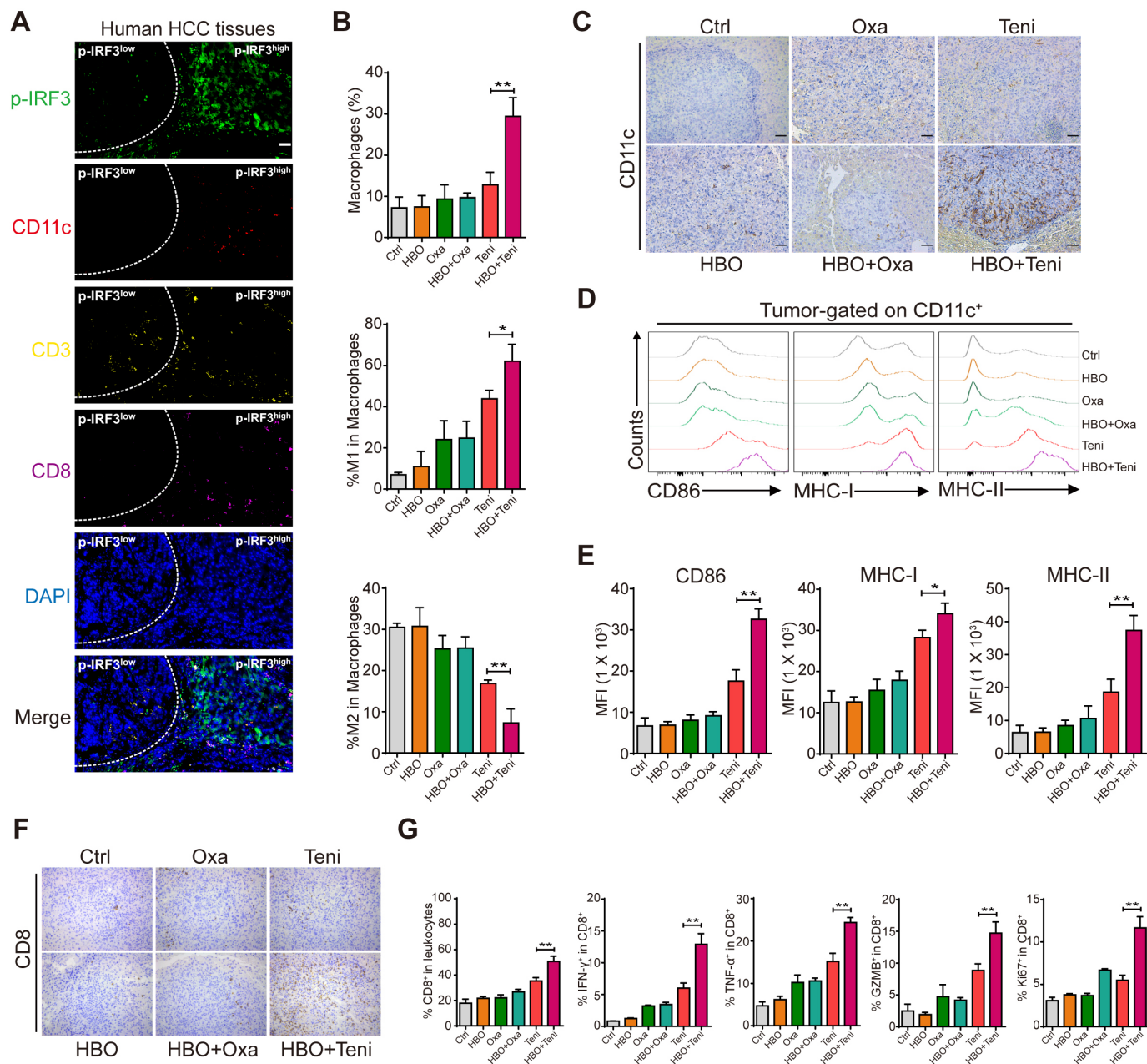
Figure 5 HBO helped teniposide to activate the antitumor response in mouse HCC tumor model. (A) Multiplex immunofluorescence staining of p-IRF3 (green), CD11c (red), CD3 (yellow), CD8 (purple) and DAPI (blue) in p-IRF3 high expression regions and adjacent p-IRF3 low expression regions of human HCC tissues. Scale bars: 50 μm. (B) Tumor-infiltrating macrophages, M1-like macrophages (CD11b$^+$F4/80$^+$/CD86$^+$) and M2-like macrophages (CD11b$^+$F4/80$^+$/CD206$^+$) of each treatment group were identified by FACS. (C) Tumor-infiltrating CD11c$^+$ cells of each treatment group were detected by immunohistochemistry. Scale bar: 50 μm. (D–E) Expression of CD86, MHC-I and MHC-II on the surface of CD11c$^+$ cells in the liver orthotopic tumor from each treatment group was detected by FACS. (F) Tumor-infiltrating CD8$^+$ cells of each treatment group were detected by immunohistochemistry. Scale bar: 50 μm. (G) Total infiltrating CD8$^+$ cells and the intracellular expression of IFN-γ, TNF-α, GZMB and Ki67 of CD8$^+$ T cells in the liver orthotopic tumor from each treatment group were detected by FACS. Data in (B), (E) and (G) are shown as mean±SD of three independent experiments. *P<0.05, **P<0.01, ***P<0.001. Ctrl, control; DAPI, 4′,6-diamidino-2-phenylindole; FACS, fluorescence-activated cell sorting; GZMB, granzyme B; HBO, hyperbaric oxygen; HCC, hepatocellular carcinoma; IFN-γ, interferon γ; IRF3, interferon regulatory factor 3; MFI, mean fluorescence intensity; MHC, major histocompatibility complex; Oxa, oxaliplatin; Teni, teniposide; TNF-α, tumor necrosis factor-α.

teniposide chemotherapy. Moreover, M1-like macrophage phenotype was significantly upregulated in tumors from the HBO+teniposide combination group, while M2-like macrophage accumulation was markedly diminished, suggesting repolarization or recruitment of macrophages

with reduced immunosuppressive capacity (figure 5B and online supplemental figure 5A,B). For DCs, IHC staining showed a significantly increased infiltration of CD11c$^+$ cells toward the tumor after HBO+teniposide treatment (figure 5C). Flow cytometry also revealed tumor-derived

DCs showed upregulated expression levels of CD86, major histocompatibility complex (MHC)-I and MHC-II molecules compared with other groups (figure 5D,E), suggesting the promotion of maturation and antigen-presenting function of DCs. These results supported that HBO could boost teniposide-induced, cGAS-STING-dependent IFN-I and NF-κB signaling activation in HCC tumor cells, which in turn recruited and activated DCs.

Second, we evaluated the profiles of tumor-infiltrating CTLs of each group. We found that HBO+teniposide also promoted CD8^{+} cell infiltration toward the tumor tissues (figure 5F,G). Furthermore, IFN-γ, tumor necrosis factor-α (TNF-α), granzyme B production and Ki67 expression by CD8^{+} T cells from the tumors that received combined HBO+teniposide treatment displayed significant increase compared with that from other treatment groups (figure 5G and online supplemental figure 5C). These results support HBO could help teniposide chemotherapy to effectively invigorate tumor-infiltrating CTLs.

Thus, the combination of HBO and teniposide treatment significantly increased the tumor infiltration of proinflammatory innate immunocytes, which finally stimulated an immunogenic, T cell-inflamed TME.

Combined HBO with teniposide chemotherapy sensitizes tumor response to anti-PD-1 immunotherapy

Encouraged by the robust cellular immunity induced by the combined HBO with teniposide treatment, we next evaluated the efficiency of this combined therapy in sensitizing tumor response to anti-PD-1 treatment. We established subcutaneous Hepa1-6 mouse tumor models, which were randomly divided into the following four groups: DMSO (Ctrl), PD-1, teniposide+PD-1 (Teni+PD-1) and HBO+teniposide+PD-1 (HBO+Teni+PD-1). The brief treatment schedule is described in figure 6A. Tumor growth of mice in the HBO+Teni+PD-1 group was significantly inhibited compared with that of the Teni+PD-1 group, indicating the combination therapy of HBO and teniposide sensitizes tumor response to anti-PD-1 treatment (figure 6B and online supplemental figure 6A). Further verification of this combined therapy on mouse colon adenocarcinoma and melanoma tumor models also demonstrated similar tumor suppressive effects (figure 6C,D and online supplemental figure 6B,C).

Collectively, these results show that HBO promoted the IFN-I and NF-κB signaling induced by teniposide chemotherapy, leading to the tumor infiltration of proinflammatory innate immunocytes and invigorated CTLs, which eventually enhanced the antitumor efficacy of anti-PD-1 immunotherapy (figure 6E).

HBO boosts teniposide-induced STING signaling toward the clinical samples

To support our previous experimental results, we also investigated if HBO promoted teniposide-induced cGAS-STING activation in clinical samples. To that end, we tested HBO and teniposide in surgically resected fresh tumor tissues from patients with HCC (online supplemental figure 6D and online supplemental table 3). Fresh tumor tissues were cut into pieces (4–6 mm) in a sterile plate. All tumor pieces were randomized into four groups and the time point was recorded as 0 hour. The groups were as follows: DMSO, HBO, teniposide (Teni) and HBO+teniposide (HBO+Teni). The DMSO and teniposide groups were persistently incubated in a hypoxic incubator (37°C, 1% O_2, 5% CO_2) to maintain the oxygen-deprived status inside the tumor. The HBO and HBO+teniposide groups received one-time HBO treatment (2.8 ATA, 2 hours) at 0 hour and were then transferred into a hypoxia incubator. At the time points of 12 and 24 hours, the HBO and HBO+teniposide groups received another two HBO treatments. All tumor samples were collected after the final HBO administration. Consistent with the findings in murine models, the expression of HIF-1α in clinical samples decreased substantially after three-time HBO treatment. Meanwhile, both teniposide-induced p-IRF3 and p-P65 activation levels were significantly enhanced, indicating HBO boosted teniposide to induce cGAS-STING signaling toward the clinical samples (figure 7A,B). As a consequence, the mRNA expression of *IFNB1*, *IFIT1*, *IFIT2*, *CCL5* and *CXCL10* was also increased markedly, indicating the superior immunostimulatory activity of the HBO+teniposide combination (figure 7C). These results were also verified in tumors from another two different patients with HCC (figure 7D–G), supporting the potential use of the HBO+teniposide combination as a strategy to increase the immunogenicity of human tumors.

DISCUSSION

Multiple studies have demonstrated direct activation of cGAS-STING axis in the TME could lead to potent tumor regression and immune response in various tumor models, indicating cGAS-STING pathway might serve as a promising therapeutic target in HCC treatment.[25 26] Because no STING agonist has been approved for clinical use so far, we resorted to promote tumor cGAS-STING signaling through the combination of existing therapeutic methods.

Theoretically, chemotherapy is a clinically feasible way to induce tumor dsDNA-cGAS-STING type I IFN signal transduction.[1] In fact, the potency of different chemotherapy agents in triggering tumor STING signaling might vary quite a lot. In this study, we verified that commonly used systemic or local chemotherapy drugs for HCC were ineffective in inducing tumor cell-intrinsic cGAS-STING activation, while the traditional topoisomerase II inhibitor, teniposide, was excellent in activating cGAS-STING-mediated IFN-I and NF-κB signaling in HCC cells. Considering the prominent immunostimulatory ability exhibited, teniposide might have some prospects in HCC treatment, especially when combined with immunotherapies.

It is widely acknowledged that hypoxic status inside the TME could aggravate tumor resistance to chemotherapy via multiple mechanisms.[27–29] Here, we illustrated another
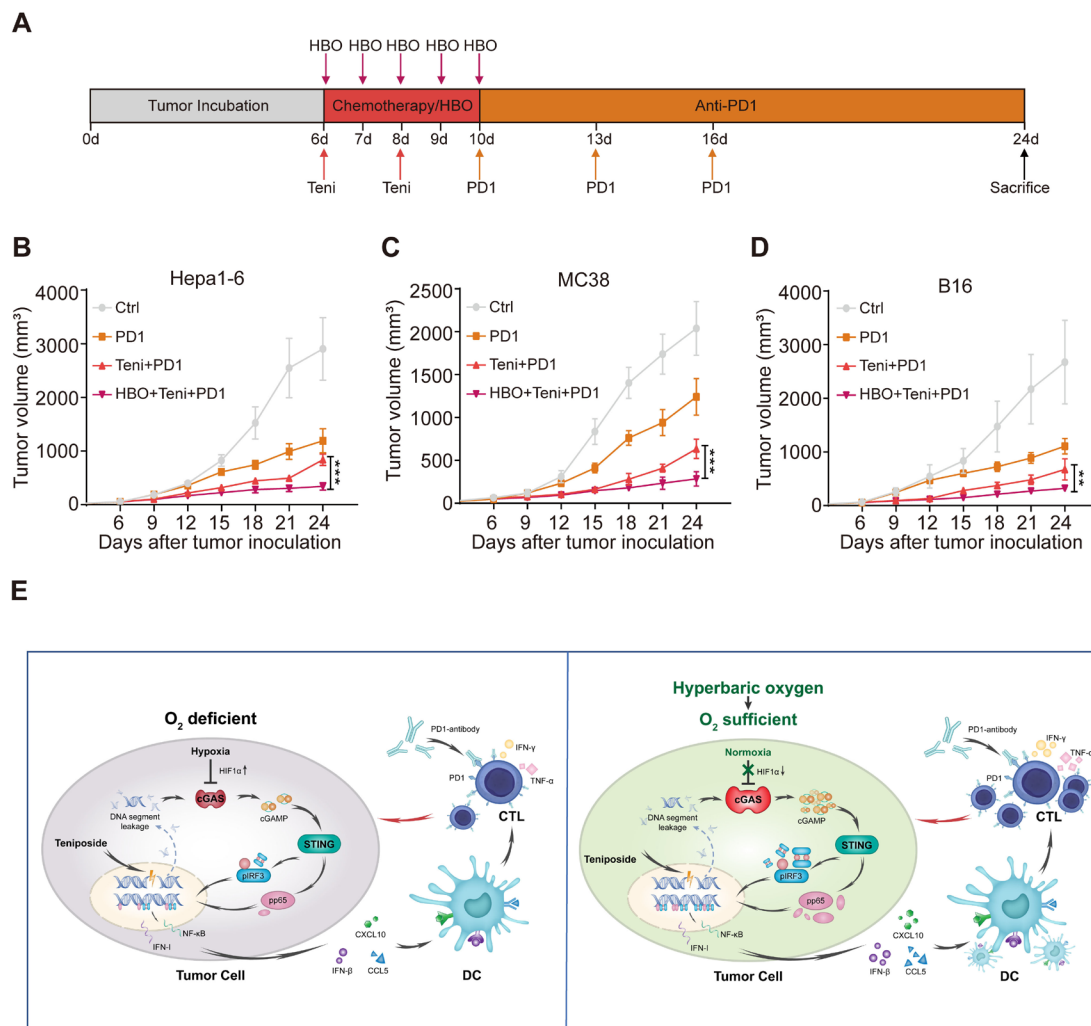
Figure 6 Combined HBO with teniposide chemotherapy sensitized tumor response to PD-1 antibody. (A) Schematic illustration of anti-PD-1 sensitization experiments in vivo. Mice with subcutaneously established tumors were intraperitoneally injected with DMSO (Ctrl) and teniposide (10 mg/kg) twice at indicated time points, and HBO therapy was administrated after teniposide chemotherapy in the HBO+teniposide+PD-1 combination group for a total of five times. PD-1 antibody (200 µg per mouse) was intraperitoneally injected every 3 days at indicated time points (n=5 per group). (B–D) Tumor growth curves of Hepa1-6 (B), MC38 (C) and B16 (D) bearing mice during anti-PD-1 sensitization experiments. (E) Schematic diagram of the combination therapy based on HBO and teniposide. *P<0.05, **P<0.01, ***P<0.001. cGAS, cyclic GMP-AMP synthase; CTL, cytotoxic T lymphocyte; Ctrl, control; DC, dendritic cell; DMSO, Dimethyl sulfoxide; HBO, hyperbaric oxygen; IFN-I, interferon type I; IFN-γ, interferon γ; IRF3, interferon regulatory factor 3; NF-κB, nuclear factor kappa-B; PD1, programmed cell death protein-1; STING, stimulator of interferon genes; Teni, teniposide; TNF-α, tumor necrosis factor-α.

negative influence of hypoxia on chemotherapy from the perspective of cGAS-STING signaling transduction. In HCC cells treated with teniposide, hypoxia inactivated the cGAS-STING-mediated IFN-I and NF-κB signaling by inducing the accumulation of HIF-1α. As HCC is a typically solid tumor that contains a large number of hypoxic regions, we sought to restore the proinflammatory innate immune signaling by alleviating tumor hypoxia.

Many studies were devoted to improving the hypoxia status inside the tumor. For example, to elevate tumor O_2 concentration by catalyzing tumor cell endogenous H_2O_2 using MnO_2 nanostructures[30][31]; to block HIF signaling by delivering HIF-1α siRNA nanocarriers into the tumors[32][33] All these efforts were undoubtedly efficient to alleviate tumor hypoxia and also showed synergistic

effects in antitumor treatment; however, many steps needed to be completed before clinical translation.[34] Recent studies focused on the role of HBO in the adjuvant treatment of cancer, confirming that HBO therapy could sensitize tumor cells to doxil chemotherapy by modulating cell cycle arrest and elevating intracellular doxil concentration.[18] Furthermore, HBO also promoted immune responses against solid tumors by enhancing PD-1 Ab delivery and subsequent T cell infiltration.[19] Based on the excellent tissue oxygenation capability of HBO, we wondered whether teniposide-induced cGAS-STING activation could be promoted after HBO administration. By reoxygenating hypoxic tumor cells in vitro, we observed the rapid rescue of cGAS expression and reactivation of teniposide-induced cGAS-STING signaling,
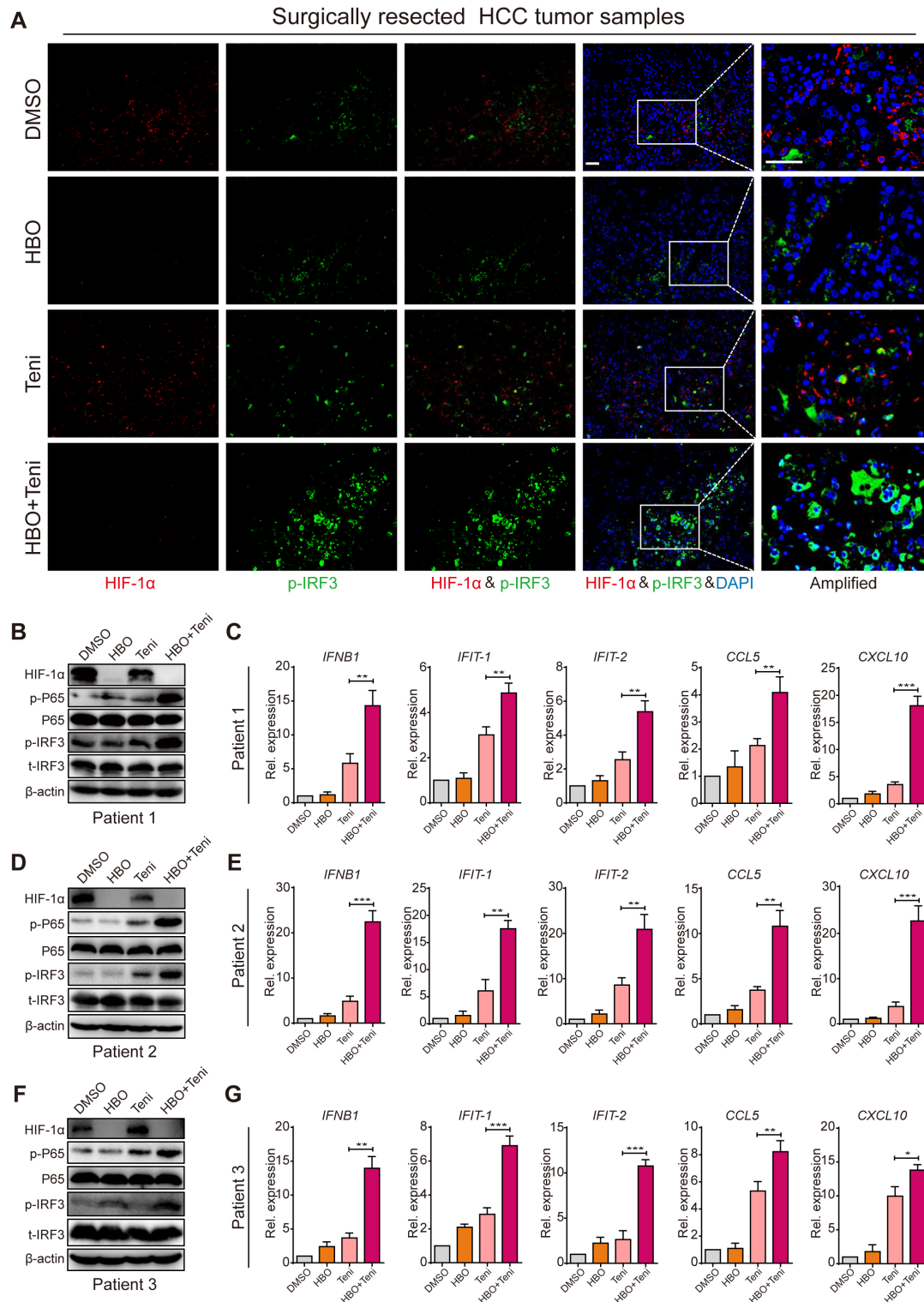
Figure 7 HBO boosted teniposide-induced cGAS-STING activation in surgically resected human HCC tumor tissues. (A) Representative immunofluorescence staining images of HIF-1α, p-IRF3 and DAPI in clinical tumor samples resected from patient 1 with HCC. Scale bar: 50 μm. (B, D, F) Clinical tumor samples were treated as in (A) and the tissular protein expression of HIF-1α, p-IRF3 and p-P65 from patient 1 (B), patient 2 (D) and patient 3 (F) was then detected by immunoblotting. (C, E, G) Clinical tumor samples were treated as in (A) and the tissular mRNA expression of *IFNB1*, *IFIT-1*, *IFIT-2*, *CCL5* and *CXCL10* from patient 1 (C), patient 2 (E) and patient 3 (G) was then measured by RT-qPCR. Data in (B), (D) and (F) are representative of three independent experiments. Data in (C), (E) and (G) are shown as mean±SD of three independent experiments. *P<0.05, **P<0.01,***P<0.001. cGAS-STING, cyclic GMP-AMP synthase-stimulator of interferon genes; DAPI, 4′,6-diamidino-2-phenylindole; DMSO, Dimethyl sulfoxide; HBO, hyperbaric oxygen; HCC, hepatocellular carcinoma; HIF-1α, hypoxia inducible factor 1α; IRF3, interferon regulatory factor 3; Rel. expression, relative expression; RT-qPCR, real time quantitative PCR; Teni, teniposide.

which provided a therapeutic basis for HBO application. By repeating HBO administration after chemotherapy in vivo, we verified the apparently higher tumor p-IRF3 expression and downstream proinflammatory signaling in the HBO+teniposide group than that in the teniposide group, indicating that HBO helped teniposide to activate cGAS-STING signaling in the Hepa1-6 mouse tumor model. Interestingly, HBO therapy did not significantly enhance p-IRF3 and downstream proinflammatory gene expression after oxaliplatin chemotherapy, which might result from the too weak cGAS-STING activation induced by oxaliplatin chemotherapy, preventing clear observation of the facilitating effect brought by HBO. Although HBO+teniposide treatment did not significantly inhibit tumor growth within a short time, survival analyses of p-IRF3, an indicator of STING activation for human patients with HCC, revealed a positive correlation between STING activation and better prognoses. Thus, a higher level of tumor STING signaling might favor the survival of patients with HCC by affecting the TME over a long time.

Further analyses of the tumor-infiltrating immune cells of each treatment group also revealed teniposide chemotherapy exhibited superior inflammatory chemotaxis compared with oxaliplatin chemotherapy. Moreover, once combined with repeated HBO treatment, tumor infiltration of M1-like macrophages and mature DCs was remarkably promoted in groups receiving teniposide chemotherapy rather than oxaliplatin. These findings were also consistent with the tumor STING activation levels in each treatment group. As T cell priming is a critical step in the activation of adaptive antitumor immunity, further evaluation regarding tumor-infiltrating T cells also revealed the amount of total CD8+ T cells and the proportion of CD8+ T cell subsets with killing functions were also enhanced by HBO after teniposide chemotherapy. The increased recruitment of invigorated cytotoxic T cells indicated the conversion of the TME from the 'cold and noninflamed' status to the 'hot and inflamed' one, which provided the TME basis for the application of ICIs.[35]

Anti-PD-1 treatment has been approved for HCC treatment for several years,[36] but the poor response rate of patients with HCC to PD-1 antibody remains a problem.[37] One possible direction for treating tumors that do not respond to ICIs is to modulate the innate immune signaling within the TME.[35] Specific to the cGAS-STING axis, cGAS itself is considered to be essential for the antitumor efficacy of ICIs,[38] while numerous studies have also demonstrated that the combination of direct STING agonists with PD-1/PD-L1 antibody shows powerful antitumor effects in animal models.[39–41] As for chemotherapy, recent animal studies have verified some chemoimmunotherapy combinations could result in potent tumor inhibition through cGAS-STING activation.[11 13] Clinically, chemotherapy might also serve as an optional way to enhance the therapeutic effect of ICIs, for clinical trials of several chemoimmunotherapies have already shown satisfactory results.[42–44] Here, we proved that repeated HBO treatments remarkably enhanced teniposide chemotherapy-induced tumor cGAS-STING signaling, which further promoted the efficacy of anti-PD-1 immunotherapy in multiple tumor models.

Until now, hepatectomy and liver transplantation are still the most effective radical treatments for patients with HCC. For patients with initially unresectable HCC, providing them a chance to receive curative resection by conducting tumor-downstaging conversion treatments was an effective way to improve survival time.[45] In recent years, with the application of ICIs in the downstaging treatment of advanced HCC, more and more patients have become eligible to receive curative surgery.[46 47] In this study, we successfully enhanced the antitumor efficacy of PD-1 antibody by combining two FDA-approved therapy. Such a triple therapy based on tumor reoxygenation and chemoimmunotherapy might support a feasible conversion therapy strategy for patients with advanced HCC. Thus, to further determine the safety and efficacy of HBO plus teniposide with subsequent PD-1 antibody in patients with unresectable HCC was of great significance in clinical translation.

It is also worth mentioning that multiple studies reported that some other therapeutic methods such as radiotherapy or DNA damage response inhibitors could also lead to the generation and accumulation of cytosolic DNA, which might trigger tumor cell cGAS activation.[1 48] This reminds us to broaden the mechanism revealed in this study by combining HBO with these dsDNA-inducing methods. So it is necessary to verify the amplification effect of HBO on the cGAS-STING-type I IFN cascade by conducting further basic or translational research in the future.

In summary, our study focused on the elevation of tumor cGAS-STING signaling in HCC. By combination of two FDA-approved therapies, we effectively stimulated an immunogenic, T cell-inflamed TME which sensitized the tumor response to anti-PD-1 treatment. These findings may enrich therapeutic ideas for advanced HCC so that we could increase the response rates of patients with HCC to anti-PD-1 immunotherapy by enhancing DNA-activated, cGAS-mediated innate immune signaling through effective tumor reoxygenation.

Author affiliations
[1]Department of Hepatic Surgery and Liver Transplantation Center, The Third Affiliated Hospital of Sun Yat-sen University, Guangzhou, Guangdong, China
[2]Vaccine Research Institute, The Third Affiliated Hospital of Sun Yat-sen University, Guangzhou, Guangdong, China
[3]Department of Biotherapy Center, The Third Affiliated Hospital of Sun Yat-sen University, Guangzhou, Guangdong, China

Competing interests None declared.

Patient consent for publication Consent obtained directly from patient(s).

Ethics approval This study involves human participants and was approved by the Ethics Review Board of The Third Affiliated Hospital, Sun Yat-sen University (approval no: 202102-137). Participants gave informed consent to participate in the study before taking part. All animal studies were approved by the Institutional Animal Care and Use Committee of South China Agricultural University (approval no: 2021D140).

Provenance and peer review Not commissioned; externally peer reviewed.

Data availability statement Data are available in a public, open access repository.

Supplemental material This content has been supplied by the author(s). It has not been vetted by BMJ Publishing Group Limited (BMJ) and may not have been peer-reviewed. Any opinions or recommendations discussed are solely those of the author(s) and are not endorsed by BMJ. BMJ disclaims all liability and responsibility arising from any reliance placed on the content. Where the content includes any translated material, BMJ does not warrant the accuracy and reliability of the translations (including but not limited to local regulations, clinical guidelines, terminology, drug names and drug dosages), and is not responsible for any error and/or omissions arising from translation and adaptation or otherwise.

ORCID iD
Linsen Ye http://orcid.org/0000-0001-9632-1949

REFERENCES

1 Yum S, Li M, Chen ZJ. Old dogs, new trick: classic cancer therapies activate cGAS. *Cell Res* 2020;30:639–48.
2 Kwon J, Bakhoum SF. The cytosolic DNA-Sensing cGAS–STING pathway in cancer. *Cancer Discov* 2020;10:26–39.
3 Galluzzi L, Vanpouille-Box C, Bakhoum SF, *et al*. Snapshot: cGAS-STING signaling. *Cell* 2018;173:276
4 Ishikawa H, Barber GN. Sting is an endoplasmic reticulum adaptor that facilitates innate immune signalling. *Nature* 2008;455:674–8.
5 Yum S, Li M, Fang Y, *et al*. Tbk1 recruitment to sting activates both IRF3 and NF-κB that mediate immune defense against tumors and viral infections. *Proc Natl Acad Sci U S A* 2021;118:e2100225118.
6 Sistigu A, Yamazaki T, Vacchelli E, *et al*. Cancer cell–autonomous contribution of type I interferon signaling to the efficacy of chemotherapy. *Nat Med* 2014;20:1301–9.
7 Yatim N, Jusforgues-Saklani H, Orozco S, *et al*. RIPK1 and NF-κB signaling in dying cells determines cross-priming of CD8 [+] T cells. *Science* 2015;350:328–34.
8 Pan B-S, Perera SA, Piesvaux JA, *et al*. An orally available non-nucleotide sting agonist with antitumor activity. *Science* 2020;369:a6098.
9 Ramanjulu JM, Pesiridis GS, Yang J, *et al*. Design of amidobenzimidazole sting receptor agonists with systemic activity. *Nature* 2018;564:439–43.
10 Shae D, Becker KW, Christov P, *et al*. Endosomolytic polymersomes increase the activity of cyclic dinucleotide sting agonists to enhance cancer immunotherapy. *Nat Nanotechnol* 2019;14:269–78.
11 Grabosch S, Bulatovic M, Zeng F, *et al*. Cisplatin-induced immune modulation in ovarian cancer mouse models with distinct inflammation profiles. *Oncogene* 2019;38:2380–93.
12 Hou L, Tian C, Yan Y, *et al*. Manganese-Based Nanoactivator Optimizes Cancer Immunotherapy *via* Enhancing Innate Immunity. *ACS Nano* 2020;14:3927–40.
13 Wang Z, Chen J, Hu J, *et al*. cGAS/STING axis mediates a topoisomerase II inhibitor–induced tumor immunogenicity. *J Clin Invest* 2019;129:4850–62.
14 Benson AB, D'Angelica MI, Abbott DE, *et al*. Hepatobiliary cancers, version 2.2021, NCCN clinical practice guidelines in oncology. *J Natl Compr Canc Netw* 2021;19:541–65.
15 Wu M-Z, Cheng W-C, Chen S-F, *et al*. miR-25/93 mediates hypoxia-induced immunosuppression by repressing cGAS. *Nat Cell Biol* 2017;19:1286–96.
16 Hanahan D. Hallmarks of cancer: new dimensions. *Cancer Discov* 2022;12:31–46.
17 Moen I, Stuhr LEB. Hyperbaric oxygen therapy and cancer—a review. *Target Oncol* 2012;7:233–42.
18 Wu X, Zhu Y, Huang W, *et al*. Hyperbaric oxygen potentiates Doxil antitumor efficacy by promoting tumor penetration and sensitizing cancer cells. *Adv. Sci.* 2018;5:1700859.
19 Liu X, Ye N, Liu S. Hyperbaric oxygen boosts PD-1 antibody delivery and T cell infiltration for augmented immune responses against solid tumors. *Adv Sci* 2021:e2100233.
20 Peng H-S, Liao M-B, Zhang M-Y, *et al*. Synergistic inhibitory effect of hyperbaric oxygen combined with sorafenib on hepatoma cells. *PLoS One* 2014;9:e100814.
21 Deng Y, Cheng J, Fu B, *et al*. Hepatic carcinoma-associated fibroblasts enhance immune suppression by facilitating the generation of myeloid-derived suppressor cells. *Oncogene* 2017;36:1090–101.
22 Qin S, Bai Y, Lim HY, *et al*. Randomized, multicenter, open-label study of oxaliplatin plus fluorouracil/leucovorin versus doxorubicin as palliative chemotherapy in patients with advanced hepatocellular carcinoma from Asia. *JCO* 2013;31:3501–8.
23 Yang X, Zhang X, Fu ML, *et al*. Targeting the tumor microenvironment with interferon-β bridges innate and adaptive immune responses. *Cancer Cell* 2014;25:37–48.
24 Zitvogel L, Galluzzi L, Kepp O, *et al*. Type I interferons in anticancer immunity. *Nat Rev Immunol* 2015;15:405–14.
25 Corrales L, Glickman LH, McWhirter SM, *et al*. Direct activation of sting in the tumor microenvironment leads to potent and systemic tumor regression and immunity. *Cell Rep* 2015;11:1018–30.
26 Thomsen MK, Skouboe MK, Boularan C, *et al*. The cGAS-STING pathway is a therapeutic target in a preclinical model of hepatocellular carcinoma. *Oncogene* 2020;39:1652–64.
27 Palazón A, Aragonés J, Morales-Kastresana A, *et al*. Molecular pathways: hypoxia response in immune cells fighting or promoting cancer. *Clin Cancer Res* 2012;18:1207–13.
28 Liang C, Dong Z, Cai X, *et al*. Hypoxia induces sorafenib resistance mediated by autophagy via activating FOXO3a in hepatocellular carcinoma. *Cell Death Dis* 2020;11.
29 Wei X, Zhao L, Ren R, *et al*. MiR-125b loss activated HIF1α/pAKT loop, leading to transarterial chemoembolization resistance in hepatocellular carcinoma. *Hepatology* 2021;73:1381–98.
30 Yang G, Xu L, Chao Y, *et al*. Hollow MnO2 as a tumor-microenvironment-responsive biodegradable nano-platform for combination therapy favoring antitumor immune responses. *Nat Commun* 2017;8.
31 Chen Q, Feng L, Liu J, *et al*. Intelligent Albumin-MnO$_2$ Nanoparticles as pH-/H$_2$O$_2$-Responsive Dissociable Nanocarriers to Modulate Tumor Hypoxia for Effective Combination Therapy. *Adv Mater* 2016;28:7129–36.
32 Masoud GN, Li W. HIF-1α pathway: role, regulation and intervention for cancer therapy. *Acta Pharm Sin B* 2015;5:378–89.
33 Chen X, Jin R, Jiang Q, *et al*. Delivery of siHIF-1α to reconstruct tumor normoxic microenvironment for effective chemotherapeutic and photodynamic anticancer treatments. *Small* 2021;17:e2100609:2100609.
34 Jayaprakash P, Vignali PDA, Delgoffe GM, *et al*. Hypoxia reduction sensitizes refractory cancers to immunotherapy. *Annu Rev Med* 2022;73:251–65.
35 Galon J, Bruni D. Approaches to treat immune hot, altered and cold tumours with combination immunotherapies. *Nat Rev Drug Discov* 2019;18:197–218.
36 El-Khoueiry AB, Sangro B, Yau T, *et al*. Nivolumab in patients with advanced hepatocellular carcinoma (CheckMate 040): an open-label, non-comparative, phase 1/2 dose escalation and expansion trial. *The Lancet* 2017;389:2492–502.
37 Sangro B, Sarobe P, Hervás-Stubbs S, *et al*. Advances in immunotherapy for hepatocellular carcinoma. *Nat Rev Gastroenterol Hepatol* 2021;18:525–43.
38 Wang H, Hu S, Chen X, *et al*. cGAS is essential for the antitumor effect of immune checkpoint blockade. *Proc Natl Acad Sci U S A* 2017;114:1637–42.
39 Reisländer T, Groelly FJ, Tarsounas M. DNA damage and cancer immunotherapy: a STING in the tale. *Mol Cell* 2020;80:21–8.

40 Iurescia S, Fioretti D, Rinaldi M. Targeting cytosolic nucleic acid-sensing pathways for cancer immunotherapies. *Front Immunol* 2018;9.

41 Fu J, Kanne DB, Leong M, *et al*. STING agonist formulated cancer vaccines can cure established tumors resistant to PD-1 blockade. *Sci Transl Med* 2015;7:252r–83.

42 Qin S, Chen Z, Liu Y, *et al*. A phase II study of anti–PD-1 antibody camrelizumab plus FOLFOX4 or GEMOX systemic chemotherapy as first-line therapy for advanced hepatocellular carcinoma or biliary tract cancer. *JCO* 2019;37:4074.

43 Chen X, Wu X, Wu H, *et al*. Camrelizumab plus gemcitabine and oxaliplatin (GEMOX) in patients with advanced biliary tract cancer: a single-arm, open-label, phase II trial. *J Immunother Cancer* 2020;8:e001240.

44 Limagne E, Thibaudin M, Nuttin L, *et al*. Trifluridine/tipiracil plus oxaliplatin improves PD-1 blockade in colorectal cancer by inducing immunogenic cell death and depleting macrophages. *Cancer Immunol Res* 2019;7:1958–69.

45 Hepatocellular carcinoma—a strategy to increase resectability. *Ann Surg Oncol* 2007;14:3301–9.

46 Finn RS, Qin S, Ikeda M, *et al*. Atezolizumab plus bevacizumab in unresectable hepatocellular carcinoma. *N Engl J Med* 2020;382:1894–905.

47 XD Z CH, YH S, *et al*. Downstaging and resection of initially unresectable hepatocellular carcinoma with tyrosine kinase inhibitor and anti-PD-1 antibody combinations. *Liver cancer* 2021;10:320–9.

48 Deng L, Liang H, Xu M, *et al*. STING-Dependent cytosolic DNA sensing promotes radiation-induced type I interferon-dependent antitumor immunity in immunogenic tumors. *Immunity* 2014;41:843–52.